Surv Geophys (2016) 37:1139–1156
DOI 10.1007/s10712-016-9385-z

Terrestrial Water Storage Anomalies Associated with Drought in Southwestern USA from GPS Observations

Shuanggen Jin[1] · **Tengyu Zhang**[1,2]

Received: 29 January 2016 / Accepted: 16 September 2016 / Published online: 30 September 2016

Abstract The Earth's surface fluid mass redistribution, e.g., groundwater depletion and severe drought, causes the elastic surface deformation, which can be measured by global positioning system (GPS). In this paper, the continuous GPS observations are used to estimate the terrestrial water storage (TWS) changes in southwestern USA, which have a good agreement with TWS changes derived from Gravity Recovery And Climate Experiment (GRACE) and hydrological models. The seasonal variation is mostly located in the Rocky mountain range and Mississippi river watershed. The largest amplitude of the seasonal variation is between 12 and 15 cm in equivalent water thickness. The timing and duration of TWS anomalies caused by the severe drought in 2012 are observed by the GPS-derived TWS, which are confirmed by the GRACE results. Different hydrological models are further used for comparison with GPS and GRACE results. The magnitude of TWS depletion from GRACE and GPS observations during the drought is larger than that from hydrological models, which indicates that the drought was caused by comparable groundwater and surface water depletion. The interannual TWS changes from GPS are also consistent with the precipitation pattern over the past 6 years, which further confirms the severe drought in 2012. This study demonstrates that continuous GPS observations have the potential as real-time drought indicator.

Keywords GPS · TWS · Drought · GRACE

✉ Shuanggen Jin
sgjin@shao.ac.cn; sg.jin@yahoo.com

[1] Shanghai Astronomical Observatory, Chinese Academy of Sciences, Shanghai 200030, China

[2] University of Chinese Academy of Sciences, Beijing 100049, China

1 Introduction

Water discharge and balance play key role in water cycle, and therefore it is critical to measure and quantify the changes in terrestrial water storage. The total terrestrial water storage (TWS) comprises the surface water, rainfall, evaporation, runoff, soil water, groundwater and other effects. Several in situ techniques have been developed to monitor TWS variations, such as soil moisture sensor, ground-penetrating radar (GPR), wireless sensor, and so on. However, the in situ measurements are focused one point measurements with high costs and strong labor intensity. Furthermore, it is hard to monitor and quantify global TWS variations with high spatial resolution due to the lack of a comprehensive global monitoring network (Jin and Feng 2013).

Recently, satellite remote sensing and satellite altimetry have been developed to monitor the water cycle, but most detect the surface water variations or just one component of TWS variations. In order to understand the land surface–atmosphere interaction and the effect of land surface processes on climate, several hydrological models have been developed by assimilating the in situ and satellite-derived water and energy components, e.g., global land data assimilation systems (GLDAS) (Rodell et al. 2004a) and WaterGAP Global Hydrology Model (WGHM) (Güntner et al. 2007). The GLDAS is a global, high-resolution and offline terrestrial modeling system with input of satellite- and ground-based observational data products using the advanced land surface modeling and data assimilation techniques, which can provide optimal near real-time fields of land surface state and flux (Rodell et al. 2004a). The WGHM has been developed to simulate variations of water storage components, which can estimate water availability in a global scale with the exception of Antarctica and Greenland at a spatial resolution of 0.5° by 0.5° (Güntner et al. 2007). The GLDAS and WGHM have been widely used for estimating global and regional hydrological cycle and spatial–temporal variations in terrestrial water storage changes as well as drought and flood monitoring. However, the GLDAS does not contain ground water component, and the WGHM does not consider water storage within the biomass and ice (including permafrost). Most important, these models have a lack of comprehensive in situ measurements.

With the launch of the Gravity Recovery And Climate Experiment (GRACE) mission in 2002, the Earth's time-variable gravity field has been determined by measuring accurately the relative positions of a pair of low Earth orbit (LEO) satellites (Tapley et al. 2004; Jin et al. 2011). By removing the effects of the atmosphere and oceans mass variations, the total terrestrial water storage (TWS) variations can thus be inferred from the observed time-variable gravity field (Wahr et al. 1998; Jin et al. 2010, 2012). Currently, the GRACE has been widely used to monitor monthly water storage variations at both global and regional scales (Jin and Feng 2013; Zhou et al. 2016). For example, Tapley et al. (2004) and Wahr et al. (2004) presented early results of the application of the GRACE products for detecting hydrological signals in different major river basins (e.g., Amazon basin and Mississippi River). Hassan and Jin (2014) used GRACE data and global hydrological models to study total water discharge in the Great Rift Valley of East Africa (i.e., Lakes Victoria, Tanganyika, and Malawi) from January 2003 to December 2012 and found significant consistent variation patters in the lake level for the three lakes with satellite altimetry. Furthermore, GRACE can monitor extreme climate events (e.g., droughts) with monthly release data (Reager and Famiglietti 2009; Long et al. 2013; Thomas et al. 2014; Castle et al. 2014). Therefore, the satellite gravimetric observations provide a unique opportunity to estimate the total water storage and its change at global and regional scales.

However, GRACE has low resolution with monthly time interval and 300–500 km spatial scale, which is not sensitive to small scale mass variations. In addition, a number of errors are existing in GRACE results, e.g., noise, aliasing errors, uncertain GIA model and leakage effects. For example, in order to get accurate TWS variations, spatial filtering functions are used to reduce the high degree noise, and the de-striping averaging filter is used for suppressing the 'N-S' striping noise in the GRACE gravity field. While the spatial averaging functions will cause the GRACE mass anomalies and leak into the outside of the region of interest, namely leakage effects, such effects can lead to aliasing errors by 40 % in glacier mass estimation from GRACE in Greenland (Jin and Zou 2015).

Water storage variations from precipitation and evaporation cause a change in surface loading. It is commonly assumed that the Earth's crust deforms elastically in response to the variations of the surface mass load. The fluid mass load change, including land water, groundwater, snow and ocean, results in the deformation on the Earth's surface. Continuous global positioning system (GPS) measurements can monitor the surface mass load change on the Earth (e.g., Sauber et al. 2000; van Dam et al. 2007; Jin et al. 2013). On the global scale, GPS coordinate time series can be used to estimate the large scale mass variations (Wu et al. 2003; Gross et al. 2004; Tregoning et al. 2009). On the other hand, the regional mass load induced deformation can also be detected by GPS coordinate time series (Amos et al. 2014; Chanard et al. 2014; Chew and Small 2014). GPS is difficult to separate the viscoelastic response to the Earth due to past deglaciation and the elastic response due to present-day ice mass loss, but the accelerating uplift rates caused by the acceleration of the ice melting can be measured by GPS. Compton et al. (2015) reported that the uplift acceleration was 1–2 mm/year^2 from 27 continuous GPS stations in Iceland, which is the reaction to the drastic climate change. The recent accelerated uplift rates were measured by GPS stations in the North Atlantic region (Jiang et al. 2010), which showed essentially ice melting at an average rate of 8.7 $\pm$ 3.5 Gt/year^2.

In addition, the displacement measured by GPS shows a good consistency with GRACE-derived deformation (Fu and Freymueller 2012; Zhang et al. 2012), which indicates that GPS has similar ability to estimate surface mass loads compared with GRACE measurement. The deformation caused by the snow, ice and water loadings above the Earth can be measured by continuous GPS observations. GPS observations on the land surface reflect the elastic response of the snow and water loadings, which can be used to estimate the snow water equivalent (SWE) (Grapenthin et al. 2006; Ouellette et al. 2013) and infer the snow or water load over local areas (Wahr et al. 2013). Continuous GPS observations of vertical land motion have been used to monitor the total water storage in California, Washington and Oregon (Argus et al. 2014; Fu et al. 2015) at a spatial resolution of approximately 50 km. Ongoing drought contributing to the reduced precipitation and streamflow can be revealed in continuous GPS time series, which makes GPS measurement as a drought indicator possible (Chew and Small 2014; Borsa et al. 2014).

The USA has suffered from the severe drought in 2012, which caused terrible damage and economic loss (Basara et al. 2013; Hoerling et al. 2014). In this paper, the recent severe drought in southwestern USA is investigated by continuous GPS observations, which are compared with GRACE TWS results and soil moisture change from hydrological models. This paper is organized as follows: in Sect. 2, theory and methods are presented. Observation data and models are introduced in Sect. 3. In Sect. 4, GPS TWS changes and responses to the drought are investigated and compared with GRACE results and hydrological models. Finally, the conclusions are given Sect. 5.

2 Theory and Methods

The mass load variations cause the deformation of the underlying Earth, which can be approximately expressed as elastic displacement based on the elastic theory (Farrell 1972). The horizontal and vertical displacements caused by the change in the mass load are measured by the continuous GPS coordinate time series. As illustrated in previous studies (Wahr et al. 2013), the vertical displacements are more sensitive to the change in mass load than horizontal displacements, which result in the larger seasonal amplitude in vertical direction. Therefore, the vertical GPS time series will be employed to investigate the TWS change. The elastic displacement can be expressed by the integration of the mass load and Green's function (Wang et al. 2012) as follows:

$$u(\theta) = \frac{\Delta M \times R}{M_e} \sum_{n=0}^{\infty} h_n P_n(\cos\theta) \tag{1}$$

where h_n is the elastic Love number, θ is the angular distance, P_n are the Legendre polynomials, R and M_e are the radius and mass of the Earth, and ΔM is the mass load. The load Love number is truncated up to 500° for the computation of the displacement, and the higher degree contributes little change in the displacement.

First, the inverted mass load will be discretized into grid cells with a spatial resolution of 0.5°. The 'edge effect' discussed in Fu et al. (2015) will be solved using a different approach in this paper. If there is only one single mass load on the surface at the known location, the pattern and amplitude of the loading can be uniquely and accurately determined by the observation of the uplift. However, the water load spreads broadly over the entire surface, and it is a non-unique problem for the inversion of the load from the uplift data. Therefore, a regularization constraint is applied to balance the model misfit and smoothness to invert the loads. The Tikhonov regularization method (Tikhonov and Arsenin 1977) is applied to estimate the surface mass water variations. We will employ the least-squares method by minimizing the following expression (Argus et al. 2014; Fu et al. 2015):

$$((Ax - b)/\sigma)^2 + \lambda(Lx)^2 \tag{2}$$

where A is the design matrix consisting of the Green's functions from Eq. (1), x is the surface mass load at each grid cell, b is the observation vector of the GPS seasonal amplitude, σ is the vector of standard errors, L is the regularization matrix (Hansen and O'Leary 1993), which will be replaced by the Laplacian operator, and λ is the regularization parameter that determines the model misfit and roughness of the neighboring disk loads. Based on the Eq. (1), the seasonal mass load distribution can be inverted from the vertical GPS annual amplitude. Therefore, it is very essential to choose a reasonable value of regularization parameter for better estimation. The trade-off curve method (Calvetti et al. 2004) will be applied to choose the parameter and more details can be found in Fu et al. (2015). A group of candidate values are evaluated in the test, and $\lambda = 2$ will be the optimal value that generates both reasonable data misfit and model roughness.

3 Observation Data and Models

3.1 Continuous GPS Observations

In order to obtain more stable and precise results for geophysical and geodynamic interpretation, a complete reprocessing of GPS data from raw observations has been developed recently. For example, high-order ionospheric effects that introduced several centimeters range bias were corrected in the reprocessing optimized strategy (Fritsche et al. 2005). As more high-precision GPS satellites orbits are utilized in IGS (International GNSS service) Analysis Centers, an improvement has greatly contributed to improve the quality and consistency of the IGS products (Steigenberger et al. 2009). With the improvement of the GPS reprocessing strategies, crustal deformation can be measured by GPS with an accuracy of millimeter level for better interpretation of the geophysical and geodynamic process. It has been almost 20 years since the GPS sites were built to measure the crustal deformation. Continuous GPS stations distributed over the southwest USA are shown in Fig. 1, ranging from 30°N to 41°N, 94°W to 115°W. The daily solutions of global GPS coordinate time series processed by GIPSY (GNSS-Inferred Positioning SYstem) are provided by Jet Propulsion Laboratory (JPL). The position time series of all continuous GPS stations are obtained from 2002 to 2014 in daily solution. The surface displacement measured as GPS coordinate time series is sensitive to the variation of the load, including the atmospheric loading. Here, the atmospheric loading was removed from the GPS coordinate time series so as to study the loading deformation caused by the hydrological cycle. According to the previous research (Tregoning and Watson 2009), the atmospheric load contributes to surface displacement with smaller amplitude when compared to the hydrological load. The deformation caused by the atmosphere can be calculated by the surface atmosphere pressure variations convolved with Green's functions. The pressure data were generally obtained from either the European Center for Medium-Range Weather Forecasts (ECMWF) (Boehm et al. 2006) or National Centers for Environment Prediction (NCEP) (Tregoning and van Dam 2005). Here, the atmosphere loadings are removed using the global surface displacement with the resolution of 2.5° from NCEP (http://geophy.uni.lu/ncep-loading.html) (van Dam 2010). The amplitude of the atmosphere effects is <1 mm

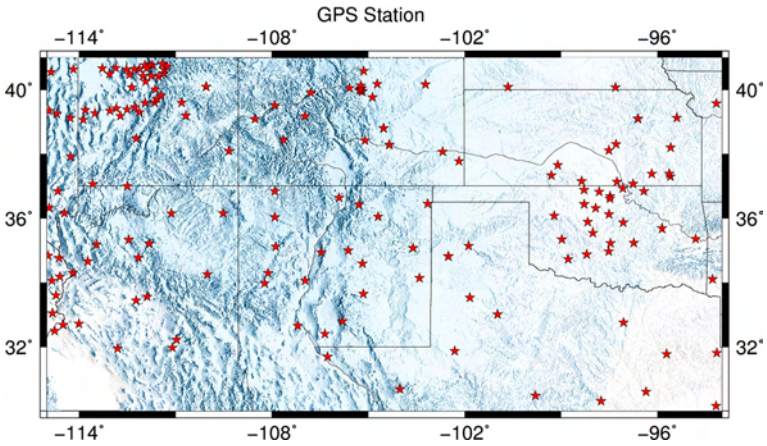

Fig. 1 GPS sites distributed in southwestern USA

in our study region. The horizontal displacement shows smaller annual amplitudes than that in the vertical, which is less sensitive to the hydrological loading change. Therefore, only vertical GPS displacements are used for the inversion.

To be consistent with GRACE TWS change for better comparison, all GPS time series in daily solutions are converted into monthly solutions. The annual amplitudes of the monthly vertical GPS time series are obtained to invert for the pattern of seasonal loadings. The vertical GPS time series are fit as follows:

$$h(t) = A_{\mathrm{a}} \cos(\omega_{\mathrm{a}} t - \varphi_{\mathrm{a}}) + A_{\mathrm{sa}} \cos(\omega_{\mathrm{sa}} t - \varphi_{\mathrm{sa}}) + vt + B + \varepsilon(t) \quad (3)$$

where $h(t)$ are vertical GPS coordinate time series, A_{a}, A_{sa} are annual amplitude and semi-annual amplitude, φ_{a}, φ_{sa} are annual phase and semi-annual phase, respectively, ω_{a}, ω_{sa} are the frequency of annual and semi-annual term as $\omega_{\mathrm{a}} = 2 * \mathrm{pi}$, $\omega_{\mathrm{sa}} = 4 * \mathrm{pi}$, respectively, v is the rate of the trend, B is constant, $\varepsilon(t)$ is residual error. The annual and semi-annual amplitudes are obtained by minimizing the total residual errors in least-squares method. The anomalous GPS sites that may be affected by the aquifers with different annual phases are not included in our inversion.

3.2 GRACE Measurements

The Gravity Recovery And Climate Experiment (GRACE) mission with more than 10 years of observations provides a unique opportunity to estimate global mass redistribution within the Earth system. Here, we employed the level 2 monthly spherical harmonic coefficients of GRACE Release 05 from the University of Texas Center for Space Research (CSR) with a truncation of up to degree 60. The monthly gravity coefficients are used by CSR from April 2002 to December 2014 (ftp://podaac-ftp.jpl.nasa.gov/allData/grace/L2/CSR/RL04/). Some missing month data are interpolated from the adjacent 2 months. The residual Stokes coefficients are obtained after removing the mean gravity field for 2002–2014. In order to reduce the systematic and correlated errors of GRACE measurements, the 300 km width of Gaussian filter and de-striping filter were applied to the GRACE observations (Swenson and Wahr 2006; Wahr et al. 2004; Jin and Feng 2013). In addition, the C_{20} component was replaced by the result from Satellite Laser Ranging data (Cheng and Tapley 2004). Due to the truncation and Gaussian filter effect, the amplitude of GRACE-inferred TWS has been attenuated on the global scale. Here, the land-grid-scaling method (Landerer and Swenson 2012) is applied. After all the corrections, the gridded TWS can be obtained in the same region as in Fig. 1, ranging from 30°N to 41°N, 94°W to 115°W. To be consistent with GPS processing strategy, the equivalent water thickness is determined by the approach of Landerer and Swenson (2012) without considering the atmosphere load effects.

3.3 Hydrological Models

The soil moisture data from North American Land Data Assimilation System (NLDAS) (Mitchell et al. 2004) and Global Land Data Assimilation System (GLDAS) (Rodell et al. 2004a) are used for comparison with GPS results. Using three different land surface models Noah, Mosaic and Variable Infiltration Capacity (VIC) as input, they will generate different models consisting of soil moisture and snow water equivalent. Regional and global spatial distribution of surface energy fluxes and states, as well as the phase of their mean diurnal cycles are included in all three models, but some differences still exist between the models and observations (Xia et al. 2012a, b). The NLDAS and GLDAS

models provide their products from 1979 to present, which specify values at 1/8° and 1° intervals of latitude and longitude, respectively. The NLDAS models assimilate observation data of North America, which provide simulation products over the USA (125° to 67°W, 25° to 53°N). The products from GLDAS are provided globally from 60°S to 90°N and 180°W to 180°E. We will obtain the soil moisture data from NLDAS and GLDAS models at the same region as in Fig. 1, ranging from 30°N to 41°N, 94°W to 115°W. The time span of the collected data is from 2002 to 2014. The magnitude of soil moisture anomalies from GLDAS has some difference from NLDAS because of different forcing data, different versions of land surface models and different spatial resolution (Long et al. 2013).

Due to the overly low snow forcing data, all three models underestimate snow water equivalent (SWE) when compared to observations. Therefore, snow water equivalent from Snow Data Assimilation System (SNODAS) that is fit to the snow telemetry (SNOTEL) measurements will be merged into NLDAS and GLDAS models for comparison (National Operational Hydrologic Remote Sensing Center 2004). The SNODAS model was developed by the National Operational Hydrologic Remote Sensing Center (NOHRSC), which provided a model estimate of snow cover for hydrological modeling and analysis. SNODAS provides estimates of snow cover and associated variables for hydrological analysis with a spatial resolution of 1/120°, ranging from 24.9504°N to 52.8754°N, 66.9421°W to 124.7337°W. The data from SNODAS will be filtered into the resolution consistent with NLDAS and GLDAS for replacing the underestimated snow water equivalent in NLDAS and GLDAS models.

3.4 Precipitation, Evapotranspiration and Runoff Data

To better understand the correlation of TWS change with precipitation accumulation, we obtain precipitation data from Parameter elevation Regressions on Independent Slopes Model (PRISM), Global Precipitation Climatology Project (GPCP) and Tropical Rainfall Measuring Mission (TRMM). The monthly estimates of precipitation obtained from PRISM data were derived by the Oregon State University's climate research initiative known as the PRISM Climate Group (Daly et al. 2008). PRISM uses point data, digital elevation model and other spatial datasets to generate gridded estimates of climatic parameters (Daly et al. 1994). PRISM provides gridded precipitation data and surface temperature at a spatial resolution of 4 km from 1981 to 2015 covering the whole USA. The precipitation data from GPCP have a spatial resolution of 2.5 degree from 1979 to present. We obtain the GPCP products in southwestern USA from 2002 to 2014. Another precipitation data set retrieved from the Tropical Rainfall Measurement Mission (TRMM) provide precipitation products from low to middle latitudes. The 3 hourly products from TRMM are used from 2002 to 2014 with a spatial resolution of 0.25 degree.

For better characterization of the TWS changes in southwestern USA, the TWS changes can be obtained by water balance equation method (Rodell et al. 2004b). The evapotranspiration data and runoff data are provided by NLDAS VIC (Variable Infiltration Capacity) model at a resolution of 1/8°. The terrestrial water budget in basin-scale can be expressed by the water balance equation as follows:

$$\partial S/\partial t = P - R - \mathrm{ET} \tag{4}$$

where ET is the evapotranspiration, P is the precipitation, R is the total basin discharge, and $\partial S/\partial t$. ∂t is total water storage change averaged over space. Here, the sampling rate is

1 month, which is consistent with the time resolution of data and models. The TWS anomalies can be obtained by integration of $\partial S/\partial t$. ∂t from January 2003 to December 2014.

4 Results and Discussion

4.1 Annual TWS Changes

The GPS data area is extended by 2° in four directions, which results in an area ranging from 28°N to 43°N, 92°W to 117°W with 251 continuous GPS stations in the extended area. The TWS is inverted in the extended region, and the annual amplitude of vertical displacement distribution is shown in Fig. 2, which is interpolated by the surface program in Generic Mapping Tools (GMT). All the GPS vertical displacements in the covered area will be employed in our inversion. GRACE TWS change and soil moisture data from hydrological models are also obtained in southwestern USA for comparison. The annual amplitudes are obtained by fitting the TWS change and soil moisture data in each grid, which are consistent with GPS-inferred results by using Eq. (3). The seasonal amplitude patterns of TWS changes from GPS, GRACE and hydrological models are shown in Fig. 3. The largest amplitude of the seasonal water storages from GPS is located in the regions within the Rocky mountain range and Mississippi river basin (Fig. 3a). The snow water in Rocky Mountain contributes to large amplitude in annual TWS change. The high precipitation and evapotranspiration rate in Mississippi river basin result in a large annual TWS change. The similar pattern can also be seen from GRACE total water storage anomalies (Fig. 3b), but with smaller amplitude due to the attenuation effects of the sampling and post-processing of GRACE observations (Landerer and Swenson 2012). GPS is more sensitive to the smaller scale water mass changes than GRACE measurements. The uncertainties of GRACE results will be discussed in details in the next section. The major

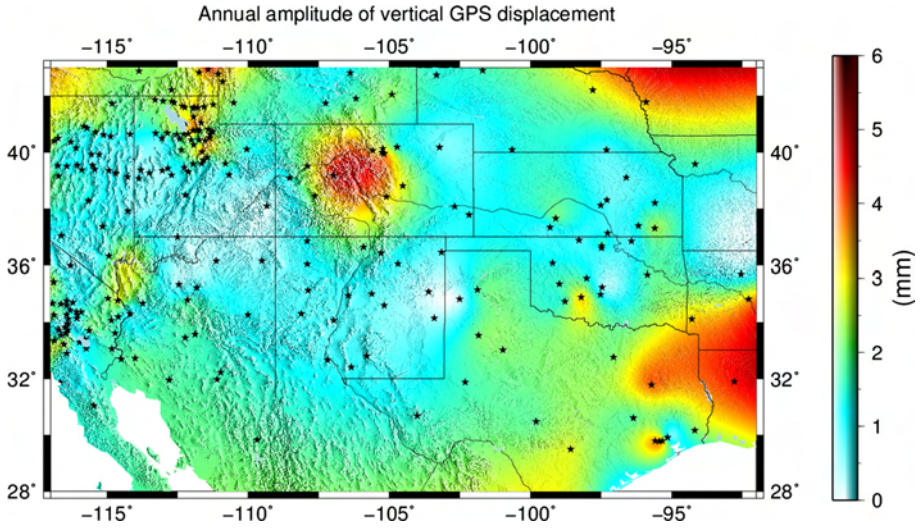

Fig. 2 Annual amplitude distribution of vertical GPS displacement in an extended region (28°N–43°N, 92°W–117°W). The annual amplitude distribution is interpolated by using GMT surface program

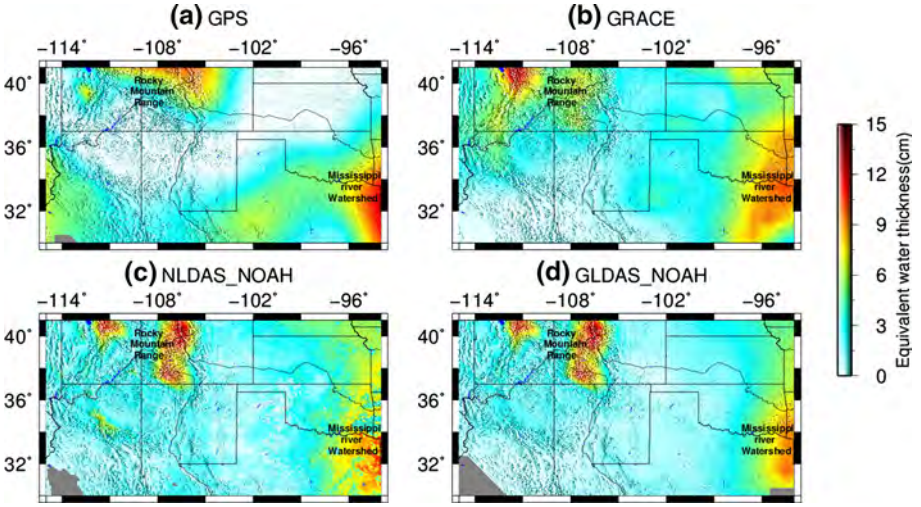

Fig. 3 Seasonal water storage changes from GPS, GRACE and soil moisture storage from NLDAS-Noah and GLDAS-Noah

component of NLDAS-Noah (Fig. 3c) and GLDAS-Noah (Fig. 3d) model comes from soil moisture storage, quite well estimating the seasonal variations in the Mississippi river watershed. Because of the underestimation of the SWE in the Rocky mountain range, the SWE data from SNODAS model have been merged with GLDAS and NLDAS models. For the qualitative evaluation of GPS-inferred water storage, the hydrological models are consistent with the inversion result in terms of magnitude and distribution. The largest amplitude of seasonal storage anomalies in these two models shows good consistency with GPS inversion water storage in Rocky mountain range and Mississippi river watershed (Fig. 3).

From GPS vertical time series, we can derive the seasonal water storage variations during spring, summer, fall and winter, which are compared with GRACE and hydrological models (Figs. 4, 5). Due to the effect of snow melt, water runoff and evaporation, the TWS change during spring and summer shows comparably larger pattern than that during fall and winter. The annual amplitude from the storage of hydrological models cannot all be revealed by GPS due to the limited GPS distribution stations.

4.2 TWS and Soil Moisture Changes During Severe Drought

4.2.1 TWS Change

The GPS vertical displacement shows elastic response to the TWS depletion as a drought indicator (Chew and Small 2014). The magnitude and spatial extent of drought in USA have been monitored. The drought monitoring system (www.droughtmonitor.unl.edu) provides drought index for the assessment of drought severity over the whole USA. The drought monitoring becomes very valuable to monitor the drought severity and extent based on simulating soil moisture. Five categories, D0-D4, of drought intensities correspond to abnormally dry through exceptional drought. Each state of the southwestern USA has suffered from the severe drought to different extents. More than 70 % of the entire area

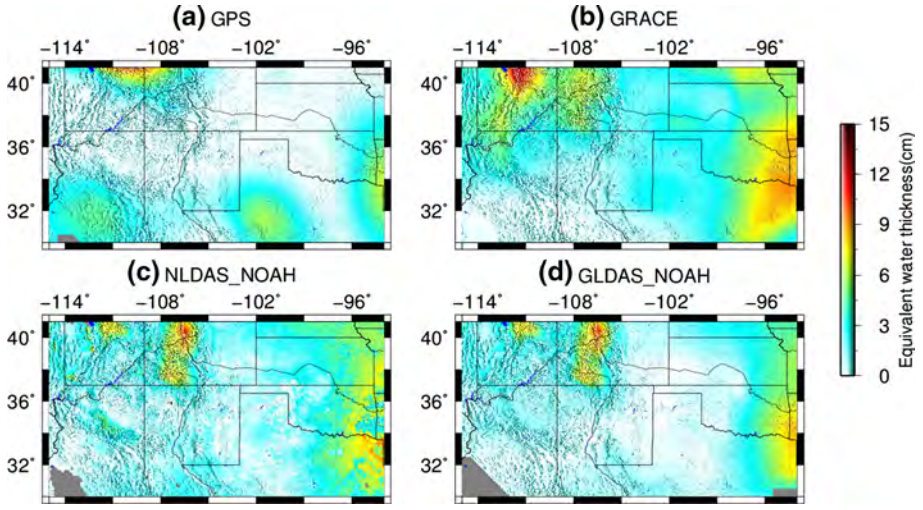

Fig. 4 Increase in seasonal water storage variations during spring and summer from **a** GPS, **b** GRACE, **c** NLDAS-Noah and **d** GLDAS-Noah

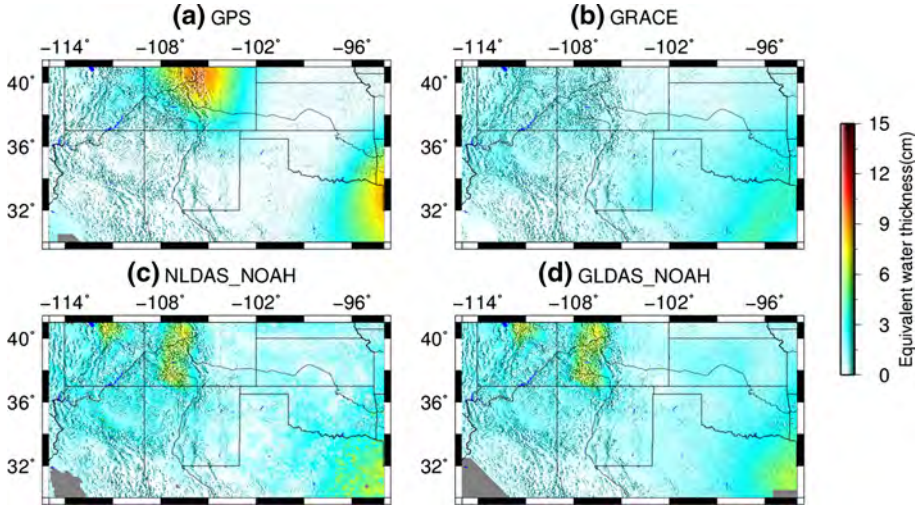

Fig. 5 Increase in seasonal water storage variations during fall and winter from **a** GPS, **b** GRACE, **c** NLDAS-Noah and **d** GLDAS-Noah

is under severe drought (D2) in 2012, which can be observed by GRACE measurement and GPS (Fig. 6). The drought starts from 2012 and increased almost steadily until 2014 with high drought intensity.

The TWS anomalies from water balance equation (WBE) method are obtained in this paper, which are compared with GPS TWS and GRACE TWS in Fig. 6. Here, the anomalies of the GPS, WBE and GRACE TWS are investigated to check whether they are consistent with the drought intensity. The velocity and constant term of each GPS time series are removed, and we obtain the GPS heights time series variations with respect to

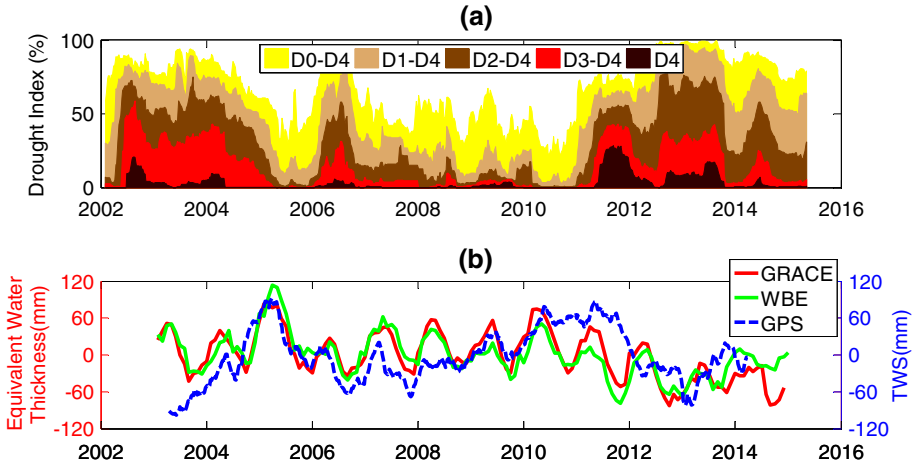

Fig. 6 **a** Drought index in southwestern USA, which means the spatial extent of the drought. Drought classification increases in severity from D0 to D4, D0 Abnormally Dry, D1 Drought-Moderate, D2 Drought-Severe, D3 Drought-Extreme, D4 Drought–Exceptional; **b** monthly TWS anomalies from GRACE (*red*) and average vertical displacement of GPS stations (*blue*)

their mean value. The GPS TWS time series are smoothed with 3-month moving-average window to reduce the high frequency fluctuations for better comparison with GRACE TWS change. First, the GRACE TWS variations during the development and recovery from the drought are discussed (Fig. 6). After the short-term recovery in early 2013, the GRACE TWS decreased again until 2014 with reaching the second minimum. The drought from 2002 to 2004 did not cause the obvious TWS depletion in GRACE measurement, but GPS measurement shows low TWS. The TWS anomalies from WBE show good consistency with GRACE results. The GRACE monthly TWS anomalies and GPS TWS change are highly correlated with each other from 2005 to 2012. The GRACE TWS decreases rapidly after 2012 as well as GPS because of drought effects. The GPS TWS shows great consistency with the drought index from the drought monitoring system. The GPS TWS is steady from 2005 to 2012 and decreases rapidly due to the drought in 2012. However, it comes to the minimum 2 months later than GRACE. Then, it has stronger recovery in early 2013.

4.2.2 Soil Moisture Changes

GRACE measures the TWS variations, including surface water reservoir water, soil moisture storage and groundwater storage. The soil moisture storage variations have high contribution to the TWS changes. The GRACE TWS anomalies are highly correlated with soil moisture storage anomalies from each hydrological model. The TWS anomalies clearly show a distinct seasonal pattern with winter peaks and summer troughs. The large interannual variability in TWS ranging from 100 mm in February 2005 to −100 mm in August 2014 indicates the wet and dry period clearly.

Due to the lack of the surface water and groundwater storage data, the amplitude of seasonal soil moisture storage from Noah, VIC and Mosaic of NLDAS and GLDAS is smaller when compared to GRACE TWS (Fig. 6). The NLDAS models have a higher spatial resolution than GLDAS models. In general, soil moisture storage anomalies in

Mosaic, VIC and Noah from NLDAS are consistent in timing and magnitude except for some extremely dry or wet periods. Soil moisture from VIC shows greater variations than Mosaic and Noah, but root-mean-square (RMS) differences between them are <10 %. The Mosaic, VIC and Noah from GLDAS also show similar soil moisture change. Because groundwater storage and surface reservoirs are not taken into account, the hydrological models underestimate the severity of the drought in 2012, which can be seen in Fig. 7. It can be concluded that the drought in 2012 has caused large amount of groundwater and surface water depletion.

4.3 Interannual TWS Change During the Severe Drought

It is a critical issue for water resource management to quantify the impact of the severe drought on the depletion of water storage. The TWS measured by GRACE is proved to be very efficient and useful to understand the impacts of the drought for better managing the restricted water resources. But it is deficient for GRACE to estimate the spatial extent and magnitude in small region with limited spatial resolution, while regional denser GPS observations have the great potential to monitor the severe drought with enough observations (Chew and Small 2014).

To investigate the spatial extent of severe drought in southwestern USA, we obtain the interannual precipitation anomalies from PRISM. The total accumulative precipitation from July to September in recent 6 years is derived to evaluate the drought, which clearly indicates the magnitude and severity of the drought because the drought is maximal during these 3 months. Figure 8 has clearly shown that the precipitation in 2011 and 2012 is extremely low when compared to other years. The average accumulative precipitation in southwestern USA is 194, 180, 190, 116, 143 and 207 mm in the recent 6 years. The accumulative precipitation in 2011 and 2012 is ~60 and ~80 % of a normal year. The Rocky mountain range receives minimum precipitation during these months.

To make a quantitative estimate of the total precipitation in southwestern US, we have analyzed monthly GPCP and TRMM data comparing with PRISM. It has been clearly

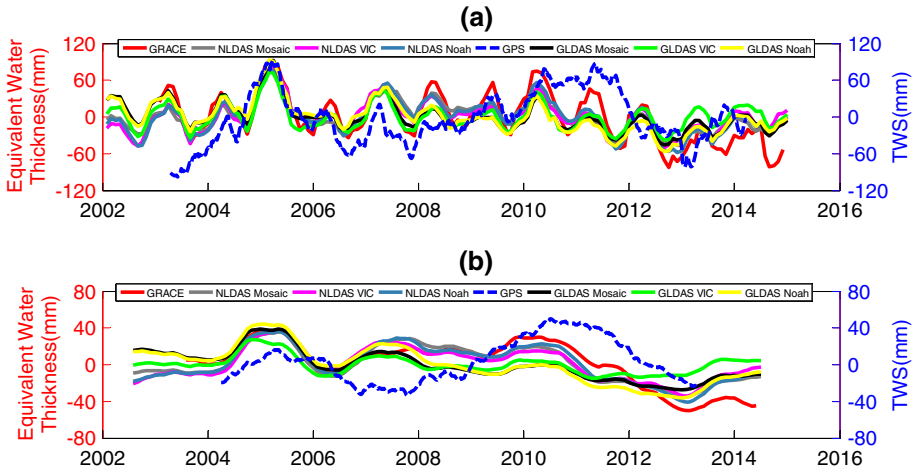

Fig. 7 **a** Monthly TWS from GRACE, NLDAS and GPS. **b** Monthly TWS from GRACE, NLDAS and GPS in southwestern USA from January 2002 to April 2014 (a filter with 6-month width is applied to show the interannual TWS change)

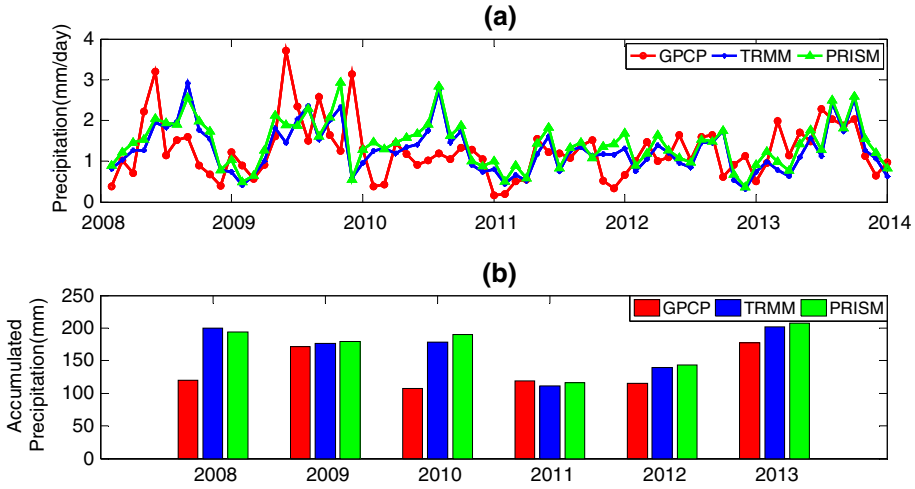

Fig. 8 **a** Monthly precipitation anomalies from GPCP (*red*), TRMM (*blue*) and PRISM (*green*); **b** accumulated precipitation in July–September from GPCP (*red*), TRMM (*blue*) and PRISM (*green*)

shown that the precipitation in 2011 and 2012 is lower than 2 mm/day, indicating two dry years in southwestern USA. And the average accumulative precipitation (July–September) from GPCP, TRMM and PRISM in 2011 and 2012 is also the lowest among the recent 6 years.

The variations of TWS derived from continuous GPS observations can monitor the effect of the drought on the water storage variation. In Fig. 9, the surface water storages from 2008 to 2013 are presented to investigate the variations of TWS, which show clear changes between each year. The interannual GPS changes (Fig. 9) are consistent with precipitation pattern in Fig. 10. The interannual precipitation variations are derived from monthly PRISM data, which are compared with the GPS-inferred surface water storage variations. The severe drought occurred in 2011 results in the reduction in the TWS, especially in Texas (Long et al. 2013). And in 2012 Utah and Colorado also suffered from the drought. The recovery in 2013 shows the end of the severe drought in southwestern US.

4.4 Uncertainties in TWS from GPS and GRACE

The main seasonal variations of GPS coordinate time series are mainly due to the redistribution of the geophysical fluid mass loads (Dong et al. 2002), but there are still unknown errors. The poroelastic effects or sediment hydrocompaction are not taken into account, and the annual amplitude of GPS sites is entirely interpreted to be hydrological loading. The systematic error and other unknown signals in the GPS time series make difficult to isolate the useful and unknown signals. One of the most important errors is GPS draconitic year with a period of 351.2 days, which have large effects on GPS annual amplitude (Ray et al. 2008; Amiri-Simkooei 2013; Griffiths and Ray 2013; Rodriguez-Solano et al. 2014). Fu et al. (2015) have made a detailed discussion about the effect of draconitic error on the inversion. On the other hand, the distribution and sparse GPS sites lead to the underestimation of TWS change in some regions. More GPS sites and longer observations can effectively solve this problem. Therefore, it still needs more work to understand and separate GPS signals for more wide applications.

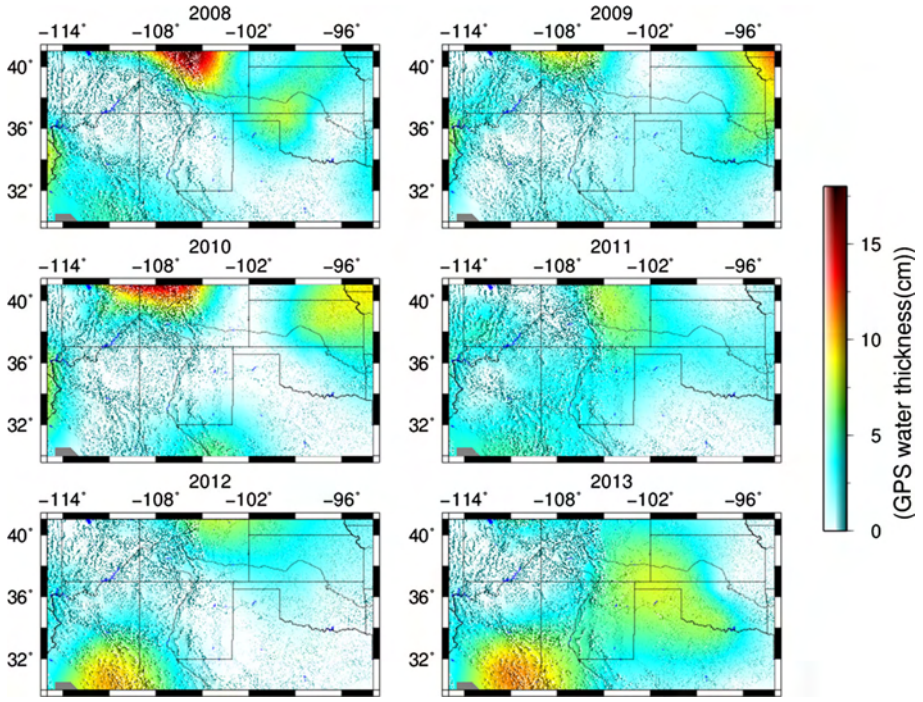

Fig. 9 Interannual water variations in recent 6 years inferred from continuous GPS vertical displacements of each year

The random errors increase as a function of spheric harmonic spectral degree in measurement errors and noise of GRACE, which results in the signal degradation of TWS estimate (Wahr et al. 2006). Several filters (Schmidt et al. 2006; Wouters and Schrama 2007) were proposed to isolate these errors, but the true geophysical signal is still unknown. Furthermore, the leakage effect is one of errors in estimating GRACE TWS change, which makes big difference in the land–ocean boundary TWS change.

5 Conclusions

In this paper, we have quantitatively estimated the terrestrial water storage variations in southwestern USA from continuous GPS measurements, which are well comparable with GRACE and hydrological models. The most seasonal water variability from GPS is located with Rocky mountain range and Mississippi river watershed, which is consistent with GRACE and hydrological models. The seasonal TWS changes revealed by GPS and GRACE show some consistency with hydrological models, but limited due to the sparse distribution of GPS sites. Furthermore, GPS can measure the severe drought in 2012 as an independent technique. The magnitudes of TWS depletion from GRACE and GPS during the drought are both larger than that from hydrological models, which indicates that the drought is caused by comparable groundwater and surface water depletion. The interannual TWS changes from GPS in recent 6 years are consistent with the pattern of precipitation from PRISM, which also indicates the severe drought in 2012. Therefore, continuous GPS

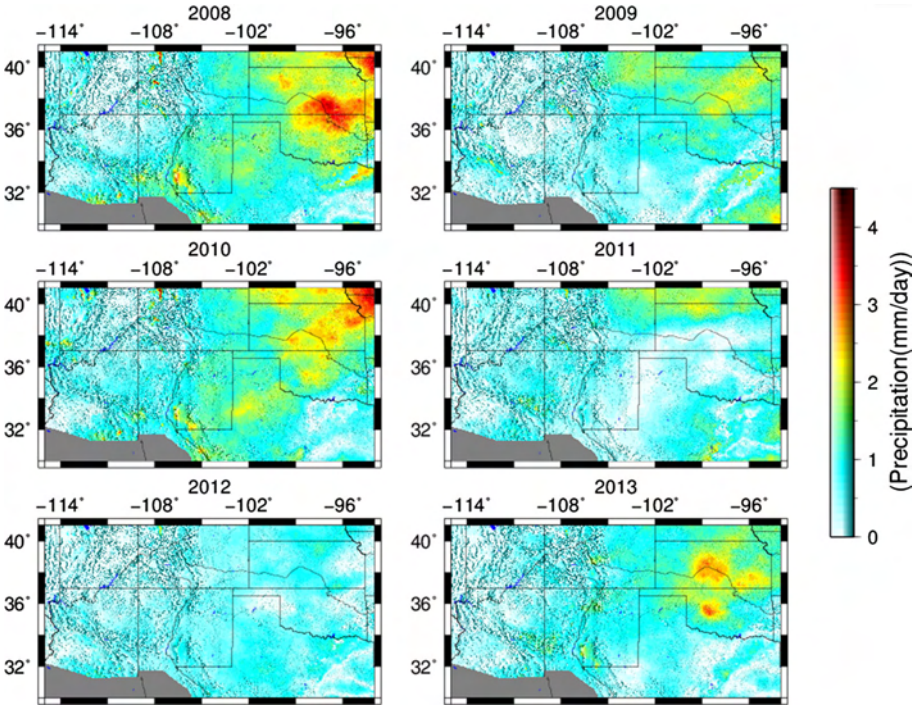

Fig. 10 Interannual precipitation variations in recent 6 years from PRISM climate group

observations have the potential to measure the drought. Although some differences in latency, sensing footprint and error source exist between GRACE and GPS time series, it is possible to combine them for drought monitoring in the future.

Acknowledgments We are grateful to JPL's GPS Analysis Center and the UNAVCO, NSF Plate Boundary Observatory, and NASA MEaSUREs projects for GPS data. The GPS data used in this study are available at ftp://sideshow.jpl.nasa.gov/pub in the directories JPL_GPS_Products and JPL_GPS_Timeseries/repro2011b. The authors would like to thank those who made GRACE observations available. The figures in this paper were plotted using the public domain Generic Mapping Tools (GMT) software (Wessel and Smith 1995). This research is supported by the National Natural Science Foundation of China (NSFC) Project (Grant No. 11373059) and Key Laboratory of Planetary Sciences, Chinese Academy of Sciences.

References

Amiri-Simkooei AR (2013) On the nature of GPS draconitic year periodic pattern in multivariate position time series. J Geophys Res Solid Earth 118:2500–2511. doi:10.1002/jgrb.50199

Amos CB, Audet P, Hammond WC, Burgmann R, Johanson IA, Blewitt G (2014) Uplift and seismicity driven groundwater depletion in central California. Nature. doi:10.1038/nature13275

Argus DF, Fu Y, Landerer FW (2014) Seasonal variation in total water storage in California inferred from GPS observations of vertical land motion. Geophys Res Lett 41:1971–1980. doi:10.1002/2014GL059570

Basara JB, Maybourn JN, Peirano CM, Tate JE, Brown PJ, Hoey JD, Smith BR (2013) Drought and associated impacts in the Great Plains of the United States—a review. Int J Geosci 4:72–81. doi:10.4236/ijg.2013.46A2009

Bevis M, Alsdorf D, Kendrick E, Fortes LP, Forsberg B, Smalley R Jr, Becker J (2005) Seasonal fluctuations in the mass of the Amazon River system and Earth's elastic response. Geophys Res Lett 32:L16308. doi:10.1029/2005GL023491

Boehm J, Werl B, Schuh H (2006) Troposphere mapping functions for GPS and very long baseline interferometry from European Centre for Medium-Range Weather Forecasts operational analysis data. J Geophys Res 111:B02406. doi:10.1029/2005JB003629

Borsa AA, Agnew DC, Cayan DR (2014) Ongoing drought-induced uplift in the western United States. Science. doi:10.1126/science.1260279

Calvetti D, Reichel L, Shuibi A (2004) L-curve and curvature bounds for Tikhonov regularization. Numer Algorithms 35:301–314

Castle SL, Thomas BF, Reager JT, Rodell M, Swenson SC, Famiglietti JS (2014) Groundwater depletion during drought threatens future water security of the Colorado River Basin. Geophys Res Lett 41:5904–5911. doi:10.1002/2014GL061055

Chanard K, Avouac JP, Ramillien G, Genrich J (2014) Modeling deformation induced by seasonal variations of continental water in the Himalaya region: sensitivity to Earth elastic structure. J Geophys Res Solid Earth 119:5097–5113. doi:10.1002/2013JB010451

Cheng M, Tapley BD (2004) Variations in the Earth's oblateness during the past 28 years. J Geophys Res 109:B09402. doi:10.1029/2004JB003028

Chew CC, Small EE (2014) Terrestrial water storage response to the 2012 drought estimated from GPS vertical position anomalies. Geophys Res Lett 41:6145–6151. doi:10.1002/2014GL061206

Compton K, Bennett RA, Hreinsdóttir S (2015) Climate-driven vertical acceleration of Icelandic crust measured by continuous GPS geodesy. Geophys Res Lett 42:743–750. doi:10.1002/2014GL062446

Daly C, Neilson RP, Phillips DL (1994) A statistical-topographic model for mapping climatological precipitation over mountainous terrain. J Appl Meteorol 33:140–158

Daly C, Halbleib M, Smith JI, Gibson WP, Doggett MK, Taylor GH, Curtis J, Pasteris PP (2008) Physiographically sensitive mapping of climatological temperature and precipitation across the conterminous United States. Int J Climatol 28(15):2031–2064

Dong D, Fang P, Bock Y, Cheng MK, Miyazaki S (2002) Anatomy of apparent seasonal variations from GPS-derived site position time series. J Geophys Res 107(B4):2075. doi:10.1029/2001JB000573

Elliott JL, Freymueller JT, Rabus B (2007) Coseismic deformation of the 2002 Denali fault earthquake: contributions from synthetic aperture radar range offsets. J Geophys Res 112:B06421. doi:10.1029/2006JB004428

Farrell WE (1972) Deformation of the Earth by surface loads. Rev Geophys 10:761–797. doi:10.1029/RG010i003p00761

Fritsche M, Dietrich R, Knofel C, Rulke A, Vey S, Rothacher M, Steigenberger P (2005) Impact of higher-order ionospheric terms on GPS estimates. Geophys Res Lett 32:L23311. doi:10.1029/2005GL024342

Fu Y, Freymueller JT (2012) Seasonal and long-term vertical deformation in the Nepal Himalaya constrained by GPS and GRACE measurements. J Geophys Res 117:B03407. doi:10.1029/2011JB008925

Fu Y, Argus DF, Landerer FW (2015) GPS as an independent measurement to estimate terrestrial water storage variations in Washington and Oregon. J Geophys Res Solid Earth. doi:10.1002/2014JB011415

Grapenthin R, Sigmundsson F, Geirsson H, Árnadóttir T, Pinel V (2006) Icelandic rhythmics: annual modulation of land elevation and plate spreading by snow load. Geophys Res Lett 33:L24305. doi:10.1029/2006GL028081

Griffiths J, Ray JR (2013) Sub-daily alias and draconitic errors in the IGS orbits. GPS Solut. doi:10.1007/s10291-012-0289-1

Gross RS, Blewitt G, Clarke PJ, Lavallée D (2004) Degree-2 harmonics of the Earth's mass load estimated from GPS and Earth rotation data. Geophys Res Lett 31:L07601. doi:10.1029/2004GL019589

Güntner A, Stuck J, Werth S, Döll P, Verzano K, Merz B (2007) A global analysis of temporal and spatial variations in continental water storage. Water Resour Res 43:W05416. doi:10.1029/2006WR005247

Hansen PC, O'Leary DP (1993) The use of the L-curve in the regularization of discrete ill-posed problems. SIAM J Sci Comput 14(6):1487–1503

Harris RA, Segall P (1987) Detection of a locked zone at depth on the Parkfield, California, segment of the San Andreas fault. J Geophys Res 92(B8):7945–7962. doi:10.1029/JB092iB08p07945

Hassan AA, Jin SG (2014) Lake level change and total water discharge in East Africa Rift Valley from satellite-based observations. Glob Planet Change 117:79–90

Hoerling M, Eischeid J, Kumar A, Leung R, Mariotti A, Mo K, Schubert S, Seager R (2014) Causes and predictability of the 2012 Great Plains drought. Bull Am Meteorol Soc 95(2):269–282. doi:10.1175/BAMS-D-13-00055.1

Houborg R, Rodell M, Li BL, Reichle R, Zaitchik BF (2012) Drought indicators based on model-assimilated Gravity Recovery and Climate Experiment (GRACE) terrestrial water storage observations. Water Resour Res 48:W07525. doi:10.1029/2011WR011291

Jiang Y, Dixon TH, Wdowinski S (2010) Accelerating uplift in the North Atlantic region as an indicator of ice loss. Nat Geosci 3:404–407. doi:10.1038/ngeo845

Jin SG, Feng GP (2013) Large-scale variations of global groundwater from satellite gravimetry and hydrological models, 2002–2012. Glob Planet Change 106:20–30. doi:10.1016/j.gloplacha.2013.02.008

Jin SG, Zhang XG (2014) A Tikhonov regularization method to estimate Earth's oblateness variations from global GPS observations. J Geodyn 79:23–29. doi:10.1016/j.jog.2014.04.011

Jin SG, Zou F (2015) Re-estimation of glacier mass loss in Greenland from GRACE with correction of land-ocean leakage effects. Glob Planet Change 135:170–178. doi:10.1016/j.gloplacha.2015.11.002

Jin SG, Chambers DP, Tapley BD (2010) Hydrological and oceanic effects on polar motion from GRACE and models. J Geophys Res 115:B02403. doi:10.1029/2009JB006635

Jin SG, Zhang LJ, Tapley BD (2011) The understanding of length-of-day variations from satellite gravity and laser ranging measurements. Geophys J Int 184(2):651–660. doi:10.1111/j.1365-246X.2010.04869.x

Jin SG, Hassan AA, Feng GP (2012) Assessment of terrestrial water contributions to polar motion from GRACE and hydrological models. J Geodyn 62:40–48. doi:10.1016/j.jog.2012.01.009

Jin SG, van Dam T, Wdowinski S (2013) Observing and understanding the Earth system variations from space geodesy. J Geodyn 72:1–10. doi:10.1016/j.jog.2013.08.001

Landerer FW, Swenson SC (2012) Accuracy of scaled GRACE terrestrial water storage estimates. Water Resour Res 48:W04531. doi:10.1029/2011WR011453

Long D, Scanlon BR, Longuevergne L, Sun A-Y, Fernando DN, Save H (2013) GRACE satellites monitor large depletion in water storage in response to the 2011 drought in Texas. Geophys Res Lett 40:3395–3401. doi:10.1002/grl.50655

Mitchell KE et al (2004) The multi-institution North American Land Data Assimilation System (NLDAS): utilizing multiple GCIP products and partners in a continental distributed hydrological modeling system. J Geophys Res 109:D07S90. doi:10.1029/2003JD003823

National Operational Hydrologic Remote Sensing Center (2004) Snow Data Assimilation System (SNODAS) data products at NSIDC, January 2002 to December 2014 Natl. Snow and Ice Data Cent., Boulder, Colo., USA. doi:10.7265/N5TB14TC

Ouellette KJ, de Linage C, Famiglietti JS (2013) Estimating snow water equivalent from GPS vertical site-position observations in the western United States. Water Resour Res 49:2508–2518. doi:10.1002/wrcr.20173

Ray J, Altamimi Z, Collieux X, van Dam T (2008) Anomalous harmonics in the spectra of GPS position estimates. GPS Solut 12:55–64. doi:10.1007/s10291-007-0067-7

Reager JT, Famiglietti JS (2009) Global terrestrial water storage capacity and flood potential using GRACE. Geophys Res Lett 36:L23402. doi:10.1029/2009GL040826

Rodell M, Houser PR, Jambor U et al (2004a) The global land data assimilation system. Bull Am Meteorol Soc 85:381–394

Rodell M, Famiglietti JS, Chen J, Seneviratne SI, Viterbo P, Holl S, Wilson CR (2004b) Basin scale estimates of evapotranspiration using GRACE and other observations. Geophys Res Lett 31:L20504. doi:10.1029/2004GL020873

Rodell M, Velicogna I, Famiglietti JS (2009) Satellite-based estimates of groundwater depletion in India. Nature 460:999–1002

Rodriguez-Solano CJ, Hugentobler U, Steigenberger P, Blobfeld M, Fritsche M (2014) Reducing the draconitic errors in GNSS geodetic products. J Geod 88:559–574. doi:10.1007/s00190-014-0704-1

Sauber J, Plafker G, Molnia BF, Bryant MA (2000) Crustal deformation associated with glacial fluctuations in the eastern Chugach Mountains, Alaska. J Geophys Res Solid Earth 105(B4):8055–8077. doi:10.1029/1999JB900433

Schmid R, Steigenberger P, Gendt G, Ge M, Rothacher M (2007) Generation of a consistent absolute phase center correction model for GPS receiver and satellite antennas. J Geod 81:781–798. doi:10.1007/s00190-007-0148-y

Schmidt M, Fengler M, Mayer-Gürr T, Eicker A, Kusche J, Sánchez L, Han SC (2006) Regional gravity modeling in terms of spherical base functions. J Geod 81:17–38. doi:10.1007/s00190-006-0101-5

Sibthorpe A, Weiss JP, Harvey N, Kuang D, Bar-Sever Y (2010) Empirical modeling of solar radiation pressure forces affecting GPS satellites. Abstract G54A-04 presented at 2010 Fall Meeting, AGU, San Francisco, Calif., 13–17 December 2010

Steigenberger P, Rothacher M, Fritsche M, Rülke A, Dietrich R (2009) Quality of reprocessed GPS satellite orbits. J Geod 83(3–4):241–248. Springer, ISSN 0949-7714. doi:10.1007/s00190-008-0228-7

Swenson SC, Wahr J (2006) Post-processing removal of correlated errors in GRACE data. Geophys Res Lett 33:L08402. doi:10.1029/2005GL025285

Tapley BD, Bettadpur S, Watkins MM, Reigber C (2004) The gravity recovery and climate experiment: mission overview and early results. Geophys Res Lett 31:L09607. doi:10.1029/2004GL019920

Thomas AC, Reager JT, Famiglietti JS, Rodell M (2014) A GRACE-based water storage deficit approach for hydrological drought characterization. Geophys Res Lett 41:1537–1545. doi:10.1002/2014GL059323

Tikhonov AN, Arsenin VY (1977) Solution of ill-posed problems. Winston & Sons, Washington. ISBN 0-470-99124-0

Tregoning P, van Dam T (2005) Atmospheric pressure loading corrections applied to GPS data at the observation level. Geophys Res Lett 32:L22310. doi:10.1029/2005GL024104

Tregoning P, Watson C (2009) Atmospheric effects and spurious signals in GPS analyses. J Geophys Res 114:B09403. doi:10.1029/2009JB006344

Tregoning P, Watson C, Ramillien G, McQueen H, Zhang J (2009) Detecting hydrologic deformation using GRACE and GPS. Geophys Res Lett 36:L15401. doi:10.1029/2009GL038718

van Dam T (2010) NCEP Derived 6 hourly, global surface displacements at 2.5 × 2.5 degree spacing. http://geophy.uni.lu/ncep-loading.html

van Dam T, Wahr J, Lavallée D (2007) A comparison of annual vertical crustal displacements from GPS and Gravity Recovery and Climate Experiment (GRACE) over Europe. J Geophys Res 112:B03404. doi:10.1029/2006JB004335

Wahr J, Molenaar M, Bryan F (1998) Time variability of the Earth's gravity field: hydrological and oceanic effects and their possible detection using GRACE. J Geophys Res 103(B12):30205–30229. doi:10.1029/98JB02844

Wahr J, Swenson S, Zlotnicki V, Velicogna I (2004) Time-variable gravity from GRACE: first results. Geophys Res Lett 31:L11501. doi:10.1029/2004GL019779

Wahr J, Swenson S, Velicogna I (2006) Accuracy of GRACE mass estimates. Geophys Res Lett 33:L06401. doi:10.1029/2005GL025305

Wahr J, Khan SA, van Dam T, Liu L, van Angelen JH, van den Broeke MR, Meertens CM (2013) The use of GPS horizontals for loading studies, with applications to northern California and southeast Greenland. J Geophys Res Solid Earth 118:1795–1806. doi:10.1002/jgrb.50104

Wang H, Xiang L, Jia L, Jiang L, Wang Z, Hu B, Gao P (2012) Load Love numbers and Green's functions for elastic Earth models PREM, iasp91, ak135, and modified models with refined crustal structure from Crust 2.0. Comput Geosci 49:190–199

Wessel P, Smith WHF (1995) New version of the generic mapping tools released. EOS Trans Am Geophys Union 76:329

Wouters B, Schrama EJO (2007) Improved accuracy of GRACE gravity solutions through empirical orthogonal function filtering of spherical harmonics. Geophys Res Lett 34:L23711. doi:10.1029/2007GL032098

Wu X, Heflin MB, Ivins ER, Argus DF, Webb FH (2003) Large-scale global surface mass variations inferred from GPS measurements of load-induced deformation. Geophys Res Lett 30(14):1742. doi:10.1029/2003GL017546

Xia Y, Mitchell KE, Ek M, Sheffield J, Cosgrove B, Wood E, Luo L, Alonge CJ, Wei H, Meng J, Livneh B, Lettenmaier D, Koren V, Duan Q, Mo K, Fan Y, Mocko D (2012a) Continental-scale water and energy flux analysis and validation for the North American Land Data Assimilation System project phase 2 (NLDAS-2): 1. Intercomparison and application of model products. J Geophys Res 117:D03109. doi:10.1029/2011JD016048

Xia Y, Mitchell KE, Ek M, Cosgrove B, Sheffield J, Luo L, Alonge CJ, Wei H, Meng J, Livneh B, Duan Q, Lohmann D (2012b) Continentalscale water and energy flux analysis and validation for North American Land Data Assimilation System Project Phase 2(NLDAS-2): 2. validation of simulated streamflow. J Geophys Res 117:D03110. doi:10.1029/2011JD016051

Zhang LJ, Jin SG, Zhang TY (2012) Seasonal variations of Earth's surface loading deformation estimated from GPS and satellite gravimetry. J Geod Geodyn 32(2):32–38

Zhou Y, Jin SG, Tenzer R, Feng J (2016) Water storage variations in the Poyang Lake basin estimated from GRACE and Satellite Altimetry. Geod Geodyn 7(2):108–116. doi:10.1016/j.geog.2016.04.003